Weak Gravitational Lensing
Part II/II

Martin Kilbinger

CEA Saclay, Irfu/SAp - AIM, CosmoStat; IAP

Euclid Summer School, Fréjus
June/July 2017

martin.kilbinger@cea.fr
www.cosmostat.org/kilbinger
Slides: http://www.cosmostat.org/ecole17

@energie_sombre #EuclidFrejus2017

Overview

Reminder from last year ...

Books, Reviews and Lecture Notes

- Bartelmann & Schneider 2001, review Weak gravitational lensing, Phys. Rep., 340, 297 arXiv:9912508
- Kochanek, Schneider & Wambsganss 2004, book (Saas Fee) Gravitational lensing: Strong, weak & micro. Download Part I (Introduction) and Part III (Weak lensing) from my homepage `http://www.cosmostat.org/kilbinger`.
- Kilbinger 2015, review Cosmology from cosmic shear observations Reports on Progress in Physics, 78, 086901, arXiv:1411.0155
- Bartelmann & Maturi 2017, review Weak gravitational lensing, Scholarpedia 12(1):32440, arXiv:1612.06535
- Henk Hoekstra 2013, lecture notes (Varenna) arXiv:1312.5981
- Sarah Bridle 2014, lecture videos (Saas Fee) `http://archiveweb.epfl.ch/saasfee2014.epfl.ch/page-110036-en.html`
- Alan Heavens, 2015, lecture notes (Rio de Janeiro) `www.on.br/cce/2015/br/arq/Heavens_Lecture_4.pdf`

Science with gravitational lensing

What has gravitational lensing ever done for us?

Part II day 1: E- and B-modes | Very brief reminders from day I

Science with gravitational lensing

Outstanding results

Dark matter is not in form of massive compact objects (MACHOs).
Microlensing rules out objects between 10^{-7} and few 10 $M_{\odot}$.

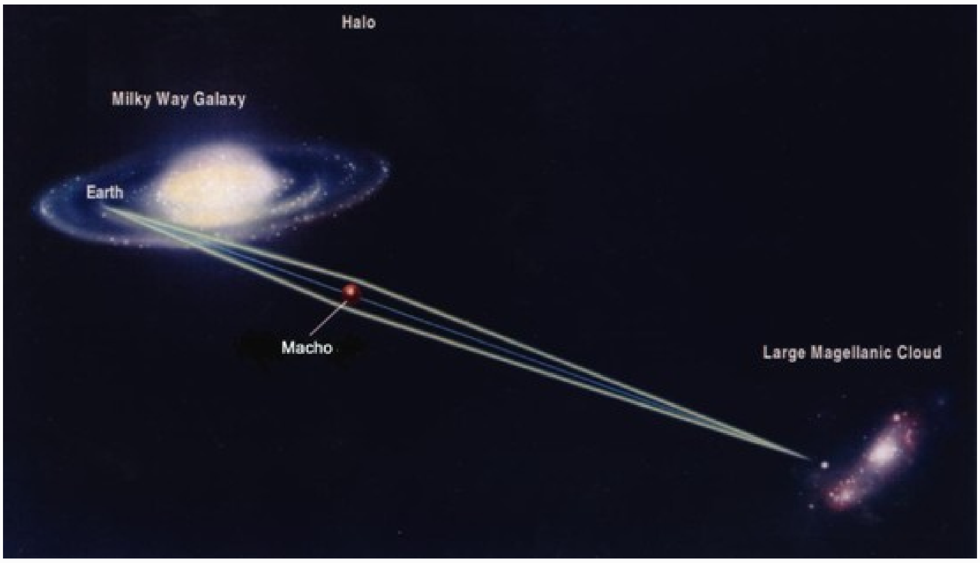

[Takahiro Sumi, Nagoya University]

Science with gravitational lensing

Outstanding results

Detection of Earth-like exoplanets with microlensing.
Masses and distances to host star similar to Earth.

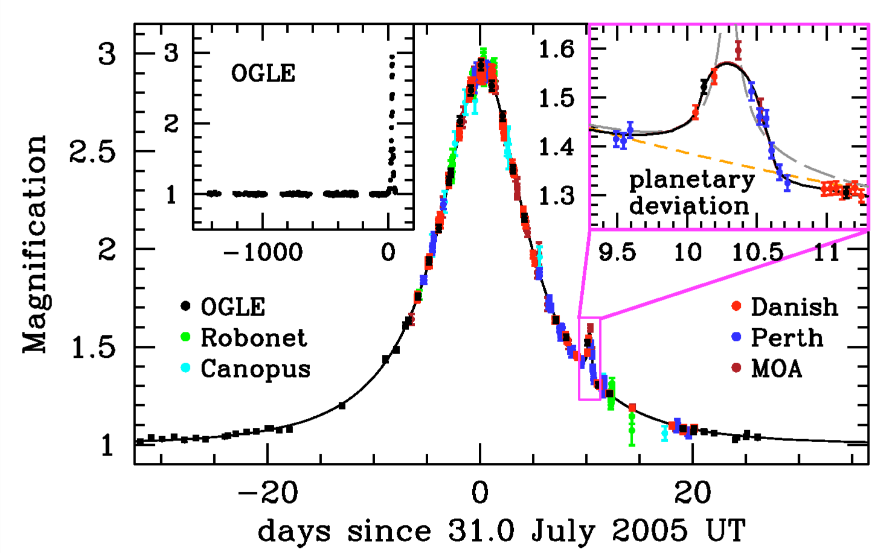

(Beaulieu et al. 2006)

Science with gravitational lensing

Outstanding results

Structure of QSO inner emission regions.
Microlensing by stars in lens galaxies.

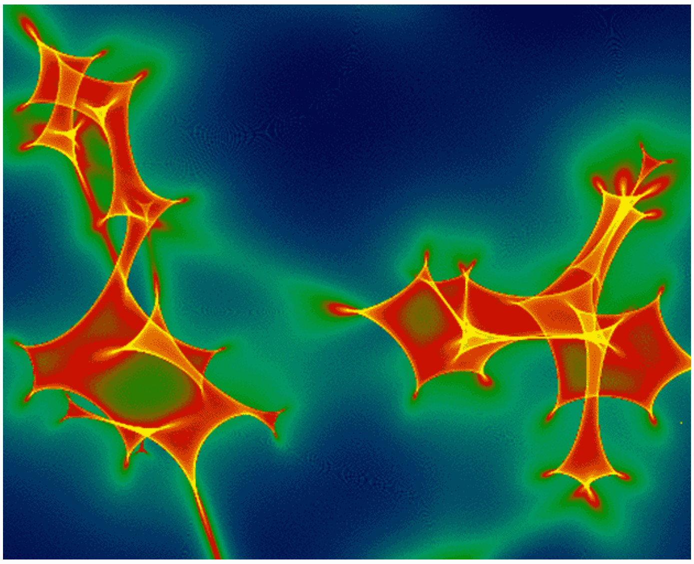

[J. Wambsganss]

Science with gravitational lensing

Outstanding results

Dark matter profiles in outskirts of galaxies.
Measuring halo mass to very large galactic scales.

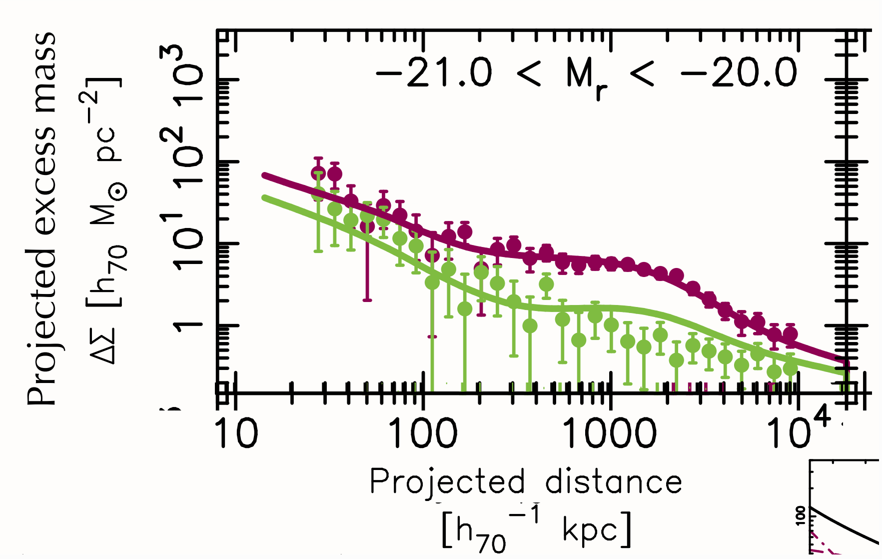

(Velander et al. 2014)

Part II day 1: E- and B-modes | Very brief reminders from day I

Science with gravitational lensing

Outstanding results

Galaxy clusters are dominated by dark matter.
Bullet cluster and others: bulk of mass is collisionless.

(Clowe et al. 2006)

Martin Kilbinger (CEA) Weak Gravitational Lensing Part II 6 / 117

Science with gravitational lensing

Outstanding results

Observation of very-high ($z \geq 7$) galaxies.
Galaxy clusters as "natural telescopes".

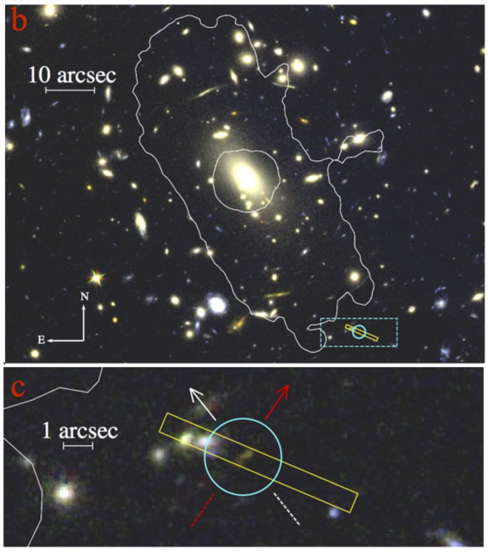

(Hoag et al. 2017)

Part II day 1: E- and B-modes Very brief reminders from day I

Science with gravitational lensing

Outstanding results

Hints of inconsistency of our cosmological model at low and high z?
Planck and WL in tension? Also WL cluster masses for Planck SZ clusters; H_0 from cepheids + SL.

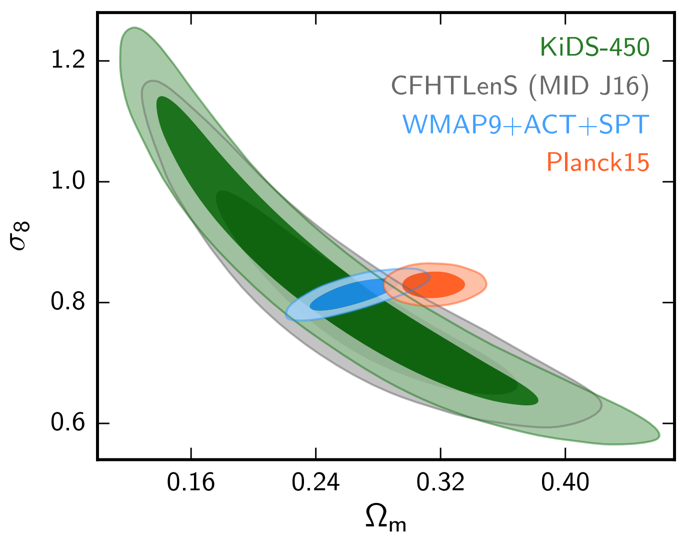

(Hildebrandt et al. 2017)

Science with gravitational lensing

Outstanding results

General relativity holds on cosmological scales.
Joint WL and galaxy clustering cosmology-independent GR test.

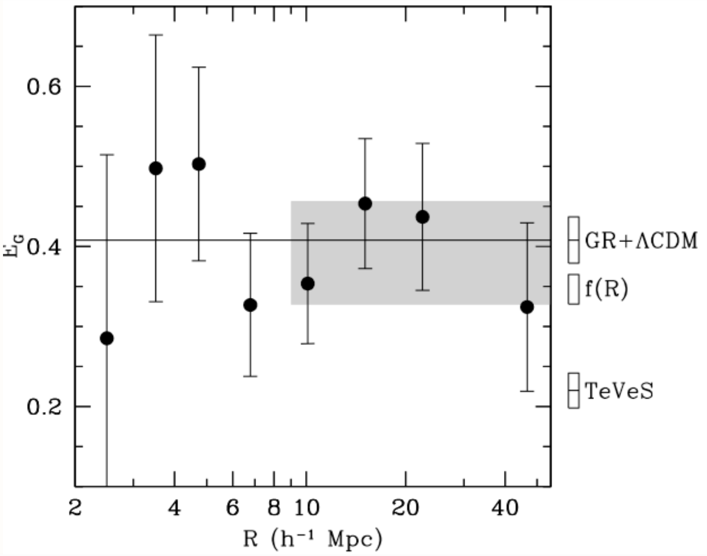

(Reyes et al. 2010)

Science with gravitational lensing

Outstanding results

Dark matter is not in form of massive compact objects (MACHOs).
Detection of Earth-mass exoplanets.
Structure of QSO inner emission regions.
Dark matter profiles in outskirts of galaxies.
Galaxy clusters are dominated by dark matter.
Observation of very-high ($z \geq 7$) galaxies.
Hints of inconsistency of our cosmological model at low and high z?
General relativity holds on cosmological scales.

Most important properties of gravitational lensing

Lensing probes total matter, baryonic + dark.
Independent of dynamical state of matter.
Independent of nature of matter.

Cosmic shear, or weak cosmological lensing

Light of distant galaxies is deflected while travelling through inhomogeneous Universe. Information about mass distribution is imprinted on observed galaxy images.

- Continuous deflection: sensitive to projected 2D mass distribution.
- Differential deflection: magnification, distortions of images.
- Small distortions, few percent change of images: need statistical measurement.
- Coherent distortions: measure correlations, scales few Mpc to few 100 Mpc.

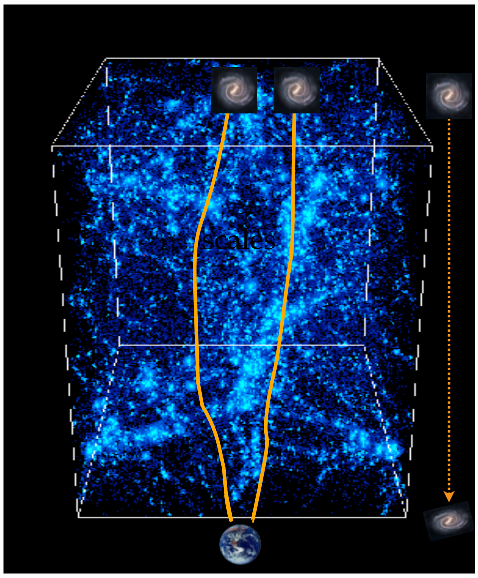

Cosmic shear deflection angle

We derived the deflection angle as integral over the potential gradient (continuous deflection along the line of sight):

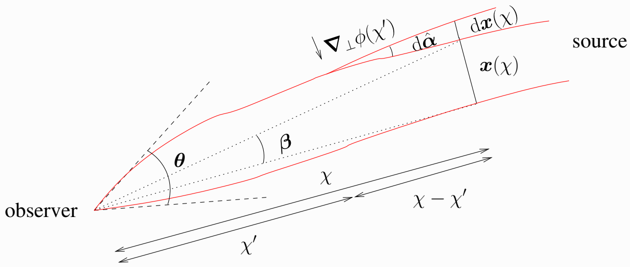

$$\boldsymbol{\alpha}(\boldsymbol{\theta}, \chi) = \frac{2}{c^2} \int_0^\chi \mathrm{d}\chi' \frac{\chi - \chi'}{\chi} \left[\boldsymbol{\nabla}_\perp \Phi(\boldsymbol{x}(\chi'), \chi') - \boldsymbol{\nabla}_\perp \Phi^{(0)}(\chi') \right].$$

Geometrical relation: (Unobervable) unlensed source position $\boldsymbol{\beta}$ is observed lensed position (direction of incoming light ray) $\boldsymbol{\theta}$ minus deflection angle $\boldsymbol{\alpha}$,

$$\boldsymbol{\beta}(\boldsymbol{\theta}, \chi) = \boldsymbol{\theta} - \boldsymbol{\alpha}(\boldsymbol{\theta}, \chi) = \boldsymbol{\theta} - \boldsymbol{\nabla}_{\boldsymbol{\theta}} \psi(\boldsymbol{\theta});$$

with the lensing potential

$$\psi(\boldsymbol{\theta}, \chi) = \frac{2}{c^2} \int_0^\chi \mathrm{d}\chi' \frac{\chi - \chi'}{\chi \chi'} \phi(\chi' \boldsymbol{\theta}, \chi').$$

Convergence and shear

The lens equation is the mapping from lens to soure 2D coordinates. The linearized lens equation

$$\frac{\partial \beta_i}{\partial \theta_j} \equiv A_{ij} = \delta_{ij} - \partial_i \partial_j \psi,$$

is described by the symmetrical 2×2 Jacobi matrix,

$$A = \begin{pmatrix} 1 - \kappa - \gamma_1 & -\gamma_2 \\ -\gamma_2 & 1 - \kappa + \gamma_1 \end{pmatrix},$$

Which defines convergence κ and shear γ.

- convergence κ: isotropic magnification
- shear γ: anisotropic stretching

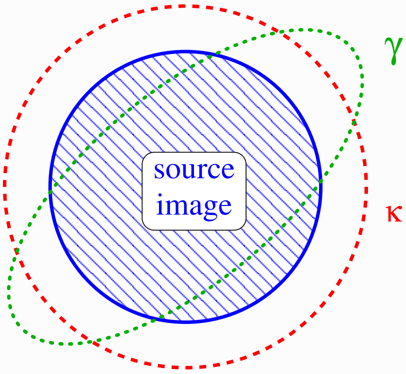

E- and B-modes: recap from part I

Shear patterns

We have seen tangential pattern in the shear field due to mass over-densities. Under-dense regions cause a similar pattern, but with opposite sign for γ. That results in radial pattern.

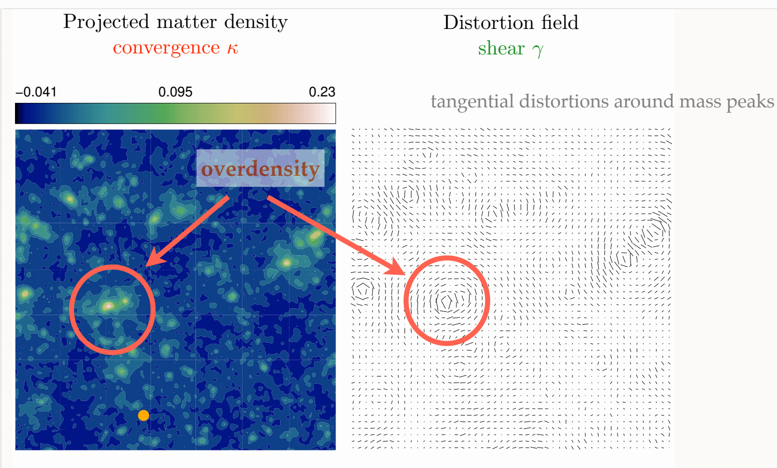

Source galaxies at $z = 1$, ray-tracing simulations by T. Hamana

E- and B-modes: recap from part I

Shear patterns

We have seen tangential pattern in the shear field due to mass over-densities. Under-dense regions cause a similar pattern, but with opposite sign for γ. That results in radial pattern.

Under idealistic conditions, these are the only possible patterns for a shear field, the E-mode. A so-called B-mode is not generated.

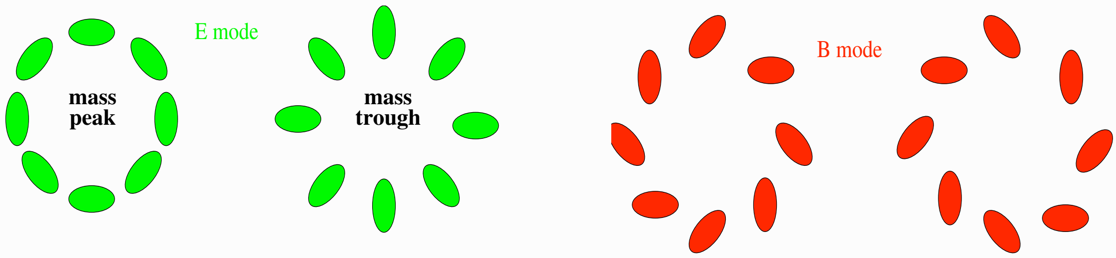

Part II day 1: E- and B-modes E-/B-mode decomposition recap

E- and B-modes: recap I

Origins of a B-mode

Measuring a non-zero B-mode in observations is usually seen as indicator of residual systematics in the data processing (e.g. PSF correction, astrometry).

Other origins of a B-mode are small, of %-level:

- Higher-order terms beyond Born appproximation (propagation along perturbed light ray, non-linear lens-lens coupling), and other (e.g. some ellipticity estimators)
- Lens galaxy selection biases (size, magnitude biases), and galaxy clustering
- Intrinsic alignment (although magnitude not well-known!)
- Varying seeing and other observational effects (table ronde topic!)
- Non-standard cosmologies (non-isotropic, TeVeS, . . .)

E- and B-modes: recap II

Measuring E- and B-modes

Separating data into E- and B-mode is not trivial.

To directly obtain $\kappa^{\rm E}$ and $\kappa^{\rm B}$ from γ, there is leakage between modes due to the finite observed field (border and mask artefacts).

One can quantify the shear pattern, e.g. with respect to reference centre points, but the tangential shear $\gamma_{\rm t}$ is not defined at the center.

Solution: filter the shear map. (= convolve with a filter function Q). This also has the advantage that the spin-2 quantity shear is transformed into a scalar.

This is equivalent to filtering κ with a function U that is related to Q.

E- and B-modes: recap III

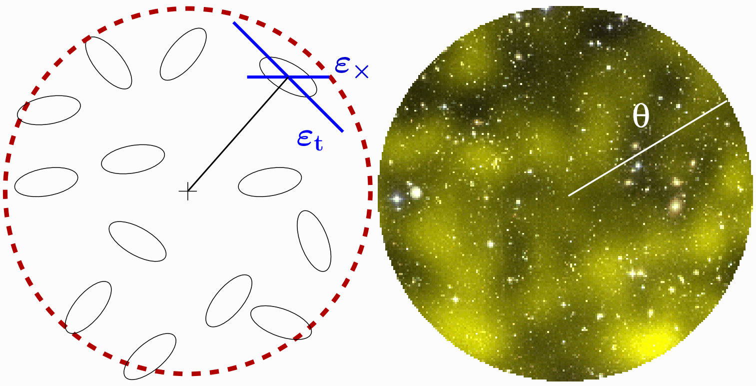

The resulting quantity is called aperture mass $M_{\rm ap}(\theta)$, which is a function of the filter size, or smoothing scale, θ. It is only sensitive to the E-mode.

If one uses the cross-component shear $\gamma_\times$ instead, the filtered quantity, $M_\times$ captures the B-mode contribution only.

End of recap from part I.

Convergence as potential field

Again convergence κ and shear γ:

$$\frac{\partial \beta_i}{\partial \theta_j} \equiv A_{ij} = \delta_{ij} - \partial_i \partial_j \psi;$$

$$A = \begin{pmatrix} 1-\kappa-\gamma_1 & -\gamma_2 \\ -\gamma_2 & 1-\kappa+\gamma_1 \end{pmatrix}.$$

From this, write κ and γ as second derivatives of the potential.

Part II day 1: E- and B-modes | E-/B-mode estimators

Convergence as potential field

Again convergence κ and shear γ:

$$\frac{\partial \beta_i}{\partial \theta_j} \equiv A_{ij} = \delta_{ij} - \partial_i \partial_j \psi;$$

$$A = \begin{pmatrix} 1-\kappa-\gamma_1 & -\gamma_2 \\ -\gamma_2 & 1-\kappa+\gamma_1 \end{pmatrix}.$$

From this, write κ and γ as second derivatives of the potential.

$$\kappa = \frac{1}{2}\left(\partial_1\partial_1 + \partial_2\partial_2\right)\psi = \frac{1}{2}\nabla^2\psi; \quad \gamma_1 = \frac{1}{2}\left(\partial_1\partial_1 - \partial_2\partial_2\right)\psi; \quad \gamma_2 = \partial_1\partial_2\psi.$$

Convergence as potential field

Again convergence κ and shear γ:

$$\frac{\partial \beta_i}{\partial \theta_j} \equiv A_{ij} = \delta_{ij} - \partial_i \partial_j \psi;$$
$$A = \begin{pmatrix} 1-\kappa-\gamma_1 & -\gamma_2 \\ -\gamma_2 & 1-\kappa+\gamma_1 \end{pmatrix}.$$

From this, write κ and γ as second derivatives of the potential.

$$\kappa = \frac{1}{2}\left(\partial_1\partial_1 + \partial_2\partial_2\right)\psi = \frac{1}{2}\nabla^2\psi; \;\; \gamma_1 = \frac{1}{2}\left(\partial_1\partial_1 - \partial_2\partial_2\right)\psi; \;\; \gamma_2 = \partial_1\partial_2\psi.$$

We can now define a vector field $\boldsymbol{u}$ for which the convergence is the "potential", with

$$\boldsymbol{u} = \boldsymbol{\nabla}\kappa.$$

Express $\boldsymbol{u}$ in terms of the shear.

Part II day 1: E- and B-modes E-/B-mode estimators

Convergence as potential field

Again convergence κ and shear γ:

$$\frac{\partial \beta_i}{\partial \theta_j} \equiv A_{ij} = \delta_{ij} - \partial_i \partial_j \psi;$$
$$A = \begin{pmatrix} 1-\kappa-\gamma_1 & -\gamma_2 \\ -\gamma_2 & 1-\kappa+\gamma_1 \end{pmatrix}.$$

From this, write κ and γ as second derivatives of the potential.

$$\kappa = \frac{1}{2}\left(\partial_1\partial_1 + \partial_2\partial_2\right)\psi = \frac{1}{2}\nabla^2\psi; \;\; \gamma_1 = \frac{1}{2}\left(\partial_1\partial_1 - \partial_2\partial_2\right)\psi; \;\; \gamma_2 = \partial_1\partial_2\psi.$$

We can now define a vector field $\boldsymbol{u}$ for which the convergence is the "potential", with

$$\boldsymbol{u} = \boldsymbol{\nabla}\kappa.$$

Express $\boldsymbol{u}$ in terms of the shear.

$$\boldsymbol{u} = \begin{pmatrix} \partial_1\kappa \\ \partial_2\kappa \end{pmatrix} = \begin{pmatrix} \frac{1}{2}(\partial_1\partial_1\partial_1 + \partial_1\partial_2\partial_2)\kappa \\ \frac{1}{2}(\partial_1\partial_1\partial_2 + \partial_2\partial_2\partial_2)\kappa \end{pmatrix} = \begin{pmatrix} \partial_1\gamma_1 + \partial_2\gamma_2 \\ -\partial_2\gamma_1 + \partial_1\gamma_2 \end{pmatrix}.$$

E- and B-mode potential, convergence, and shear I

Thus, from a shear field γ, to linear order, the corresponding convergence is derived from a gradient field $\boldsymbol{u}$, and is curl-free, $\boldsymbol{\nabla} \times \boldsymbol{u} = \partial_1 u_2 - \partial_2 u_1 = 0$, as can easily be seen.
This is the E-mode, in analogy to the electric field.

However, in reality, from an observed shear field, one might measure a non-zero curl component.
This is called the B-mode, in analogy to the magnetic field.

Definition:

$$\nabla^2 \kappa^{\mathrm{E}} := \boldsymbol{\nabla} \cdot \boldsymbol{u};$$
$$\nabla^2 \kappa^{\mathrm{B}} := \boldsymbol{\nabla} \times \boldsymbol{u},$$

and potentials

$$\nabla^2 \psi^{\mathrm{E,B}} = 2\kappa^{\mathrm{E,B}}.$$

Note that ψ^{B} and κ^{B} do not correspond to physical mass over-densities.

E- and B-mode potential, convergence, and shear II

These can be written in complex notation,

$$\psi = \psi^{\mathrm{E}} + \mathrm{i}\psi^{\mathrm{B}}; \qquad \kappa = \kappa^{\mathrm{E}} + \mathrm{i}\kappa^{\mathrm{B}},$$

and the shear

$$\gamma_1 + \mathrm{i}\,\gamma_2 = \frac{1}{2}\left(\partial_1\partial_1\psi^{\mathrm{E}} - \partial_2\partial_2\psi^{\mathrm{E}}\right) - \partial_1\partial_2\psi^{\mathrm{B}} + \mathrm{i}\left[\partial_1\partial_2\psi^{\mathrm{E}} + \frac{1}{2}\left(\partial_1\partial_1\psi^{\mathrm{B}} - \partial_2\partial_2\psi^{\mathrm{B}}\right)\right].$$

Now, we can compute the E-, B-, and mixed EB-mode power spectrum.

$$\langle \hat\kappa^{\mathrm{E}}(\boldsymbol{\ell})\hat\kappa^{\mathrm{E}}(\boldsymbol{\ell}')\rangle = (2\pi)^2 \delta_{\mathrm{D}}(\boldsymbol{\ell} - \boldsymbol{\ell}') P_\kappa^{\mathrm{E}}(\ell),$$
$$\langle \hat\kappa^{\mathrm{B}}(\boldsymbol{\ell})\hat\kappa^{\mathrm{B}}(\boldsymbol{\ell}')\rangle = (2\pi)^2 \delta_{\mathrm{D}}(\boldsymbol{\ell} - \boldsymbol{\ell}') P_\kappa^{\mathrm{B}}(\ell),$$
$$\langle \hat\kappa^{\mathrm{E}}(\boldsymbol{\ell})\hat\kappa^{\mathrm{B}}(\boldsymbol{\ell}')\rangle = (2\pi)^2 \delta_{\mathrm{D}}(\boldsymbol{\ell} - \boldsymbol{\ell}') P_\kappa^{\mathrm{EB}}(\ell),$$

and can derive (from $\hat\gamma(\boldsymbol{\ell}) = \mathrm{e}^{2\mathrm{i}\beta}\hat\kappa(\boldsymbol{\ell})$, see last years' TD) for the correlators of γ in Fourier space

$$\langle \hat\gamma(\boldsymbol{\ell})\hat\gamma^*(\boldsymbol{\ell}')\rangle = (2\pi)^2 \delta_{\mathrm{D}}(\boldsymbol{\ell} - \boldsymbol{\ell}') \left[P_\kappa^{\mathrm{E}}(\ell) + P_\kappa^{\mathrm{B}}(\ell)\right],$$
$$\langle \hat\gamma(\boldsymbol{\ell})\hat\gamma(\boldsymbol{\ell}')\rangle = (2\pi)^2 \delta_{\mathrm{D}}(\boldsymbol{\ell} + \boldsymbol{\ell}')\mathrm{e}^{4\mathrm{i}\beta} \left[P_\kappa^{\mathrm{E}}(\ell) - P_\kappa^{\mathrm{B}}(\ell) + 2\mathrm{i}P_\kappa^{\mathrm{EB}}(\ell)\right].$$

Real-space correlation function (2PCF)

Fourier-transforming the last two expressions results in shear two-point correators in real space,

$$\langle \gamma(\boldsymbol{\theta}) \gamma^*(\boldsymbol{\theta} + \boldsymbol{\vartheta}) \rangle = \langle \gamma\gamma^* \rangle(\boldsymbol{\vartheta}) = \mathcal{F}\left[\langle \hat\gamma(\boldsymbol{\ell}) \hat\gamma^*(\boldsymbol{\ell}') \rangle \right](\boldsymbol{\vartheta});$$
$$\langle \gamma\gamma \rangle(\boldsymbol{\vartheta}) = \mathcal{F}\left[\langle \hat\gamma(\boldsymbol{\ell}) \hat\gamma(\boldsymbol{\ell}') \rangle \right](\boldsymbol{\vartheta});$$

But these correlators are very closely related to the shear two-point correlation functions ξ_+ and ξ_-, that we defined on day 1 (part I):

$$\xi_+(\vartheta) = \langle \gamma_{\rm t}\gamma_{\rm t} \rangle(\vartheta) + \langle \gamma_\times\gamma_\times \rangle(\vartheta)$$
$$\xi_-(\vartheta) = \langle \gamma_{\rm t}\gamma_{\rm t} \rangle(\vartheta) - \langle \gamma_\times\gamma_\times \rangle(\vartheta)$$

Recall: 2PCF

Correlation of the shear at two points yields four quantities

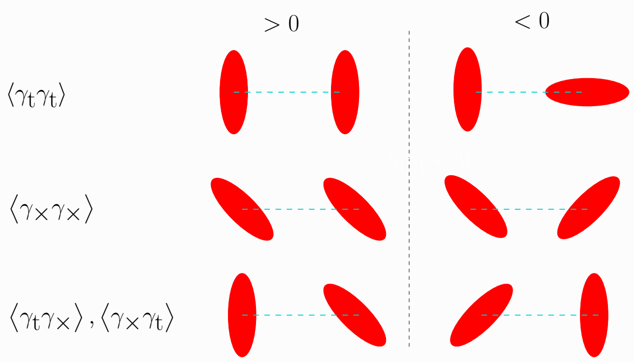

Parity conservation $\longrightarrow \langle \gamma_{\rm t}\gamma_\times \rangle = \langle \gamma_\times\gamma_{\rm t} \rangle = 0$

The two components of the shear two-point correlation function (2PCF) are defined as

$$\xi_+(\vartheta) = \langle \gamma_{\rm t}\gamma_{\rm t} \rangle(\vartheta) + \langle \gamma_\times\gamma_\times \rangle(\vartheta)$$
$$\xi_-(\vartheta) = \langle \gamma_{\rm t}\gamma_{\rm t} \rangle(\vartheta) - \langle \gamma_\times\gamma_\times \rangle(\vartheta)$$

Due to statistical isotropy & homogeneity, these correlators only depend on ϑ.

Real-space correlation function (2PCF)

Fourier-transforming the last two expressions results in shear two-point correators in real space,

$$\langle \gamma(\boldsymbol{\theta}) \gamma^*(\boldsymbol{\theta} + \boldsymbol{\vartheta}) \rangle = \langle \gamma\gamma^* \rangle(\boldsymbol{\vartheta}) = \mathcal{F}\left[\langle \hat\gamma(\boldsymbol{\ell}) \hat\gamma^*(\boldsymbol{\ell}') \rangle \right](\boldsymbol{\vartheta});$$
$$\langle \gamma\gamma \rangle(\boldsymbol{\vartheta}) = \mathcal{F}\left[\langle \hat\gamma(\boldsymbol{\ell}) \hat\gamma(\boldsymbol{\ell}') \rangle \right](\boldsymbol{\vartheta});$$

But these correlators are very closely related to the shear two-point correlation functions ξ_+ and ξ_-, that we defined on day 1 (part I):

$$\xi_+(\vartheta) = \langle \gamma_\mathrm{t} \gamma_\mathrm{t} \rangle (\vartheta) + \langle \gamma_\times \gamma_\times \rangle (\vartheta)$$
$$\xi_-(\vartheta) = \langle \gamma_\mathrm{t} \gamma_\mathrm{t} \rangle (\vartheta) - \langle \gamma_\times \gamma_\times \rangle (\vartheta)$$

Choose $\boldsymbol{\vartheta} = (\vartheta, 0)$. Then, $\gamma_\mathrm{t} = -\gamma_1$ and $\gamma_\mathrm{x} = -\gamma_2$.

$$\to \langle \gamma\gamma^* \rangle = \langle \gamma_1\gamma_1 \rangle + \langle \gamma_2\gamma_2 \rangle = \xi_+;$$
$$\langle \gamma\gamma \rangle = \langle \gamma_1\gamma_1 \rangle - \langle \gamma_2\gamma_2 \rangle + 2\mathrm{i}\langle \gamma_1\gamma_2 \rangle = \xi_- + 2\mathrm{i}\xi_\times.$$

2PCF and E-/B-mode power spectra I

We generalize the relation between 2PCF and convergence power spectrum P_κ from day 1,

$$\xi_+(\vartheta) = \frac{1}{2\pi} \int_0^\infty \mathrm{d}\ell \, \ell \mathrm{J}_0(\ell\vartheta) P_\kappa(\ell)$$
$$\xi_-(\vartheta) = \frac{1}{2\pi} \int_0^\infty \mathrm{d}\ell \, \ell \mathrm{J}_4(\ell\vartheta) P_\kappa(\ell),$$

to include E- and B-mode power spectra:

$$\xi_+(\vartheta) = \frac{1}{2\pi} \int_0^\infty \mathrm{d}\ell \, \ell \mathrm{J}_0(\ell\vartheta) \left[P_\kappa^\mathrm{E}(\ell) + P_\kappa^\mathrm{B}(\ell) \right]$$
$$\xi_-(\vartheta) = \frac{1}{2\pi} \int_0^\infty \mathrm{d}\ell \, \ell \mathrm{J}_4(\ell\vartheta) \left[P_\kappa^\mathrm{E}(\ell) - P_\kappa^\mathrm{B}(\ell) \right]$$

(and we don't look any further at $\xi_\times$, which vanished for a parity-symmetric universe.)

2PCF and E-/B-mode power spectra II

We have thus two observables (ξ_+, ξ_-) and two unknowns $(P_\kappa^{\rm E}, P_\kappa^{\rm B})$. Surely, these two power spectra can be deduced from the observations?
The above equations can be inverted using the orthogonality of the Bessel function:

$$\int_0^\infty {\rm d}\vartheta \, \vartheta {\rm J}_\nu(\ell\vartheta){\rm J}_\nu(\ell'\vartheta) = \frac{\delta_{\rm D}(\ell - \ell')}{\ell},$$

(or, alternatively, go back to the 2D Fourier integrals and use the orthogonality of the plane wave basis functions $\exp({\rm i}\boldsymbol{\ell}\boldsymbol{\vartheta})$)
resulting in

$$P_\kappa^{\rm E}(\ell) = \pi \int_0^\infty {\rm d}\vartheta \, \vartheta \left[\xi_+(\vartheta){\rm J}_0(\ell\vartheta) + \xi_-(\vartheta){\rm J}_4(\ell\vartheta)\right],$$

$$P_\kappa^{\rm B}(\ell) = \pi \int_0^\infty {\rm d}\vartheta \, \vartheta \left[\xi_+(\vartheta){\rm J}_0(\ell\vartheta) - \xi_-(\vartheta){\rm J}_4(\ell\vartheta)\right].$$

So, in principle, the E-/ and B-mode power spectra can be computed separately, but not in practice, since this requires information about the shear correlation that is unobservable, towards 0 and ∞ separation.
$\to$ We have to further filter the field for a better separation.

Aperture-mass

A few slides ago we introduced the aperture-mass as convolution of the shear field with a filter Q,

$$M_{\rm ap}(\theta, \boldsymbol{\vartheta}) = \int {\rm d}^2\vartheta' \, Q_\theta(|\boldsymbol{\vartheta} - \boldsymbol{\vartheta}'|) \, \gamma_{\rm t}(\boldsymbol{\vartheta}')$$

and claimed that this was equivlaent of convolving the convergence with another filter U,

$$M_{\rm ap}(\theta, \boldsymbol{\vartheta}) = \int {\rm d}^2\vartheta' \, U_\theta(|\boldsymbol{\vartheta} - \boldsymbol{\vartheta}'|) \, \kappa^{\rm E}(\boldsymbol{\vartheta}'), \qquad (1)$$

(Kaiser et al. 1994, Schneider 1996).

Exercise for next session (where you'll need stuff from today's TD): What is the relation between U and Q?

Convolution with shear

Parenthesis:

Eq. (3) involves the tangential shear $\gamma_{\rm t}$ with respect to the aperture centre $\boldsymbol{\vartheta}$; it should be written $\gamma_{\rm t}(\boldsymbol{\vartheta}, \boldsymbol{\vartheta}')$.
This "field" $\gamma_{\rm t}$ is thus defined locally, and cannot be represented globally.
How can this expression be written as convolution with $\gamma = \gamma_1 + {\rm i}\gamma_2$?

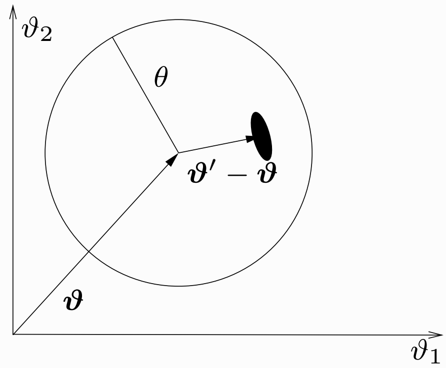

Solution:

$$\gamma_{\rm t}(\boldsymbol{\vartheta}, \boldsymbol{\vartheta}') = -\Re\left(\gamma {\rm e}^{-2{\rm i}\varphi}\right) = -\Re\left(\gamma {\rm e}^{-2{\rm i}\arctan|\vartheta_2 - \vartheta_2'|/|\vartheta_1 - \vartheta_1'|}\right)$$

$$\to M_{\rm ap}(\theta, \boldsymbol{\vartheta}) = -\Re \int {\rm d}^2\vartheta' \, \gamma(\boldsymbol{\vartheta}') {\rm e}^{-2{\rm i}\arctan[|\vartheta_2 - \vartheta_2'|/|\vartheta_1 - \vartheta_1'|]}$$

$$= \Re\left(Q_\theta' * \gamma\right)(\boldsymbol{\vartheta})$$

$$\text{with} \quad Q_\theta'(\boldsymbol{\vartheta}) = -Q_\theta(\boldsymbol{\vartheta}) {\rm e}^{-2{\rm i}\arctan[\vartheta_2/\vartheta_1]}.$$

E-/B-mode separation with $M_{\rm ap}$ I

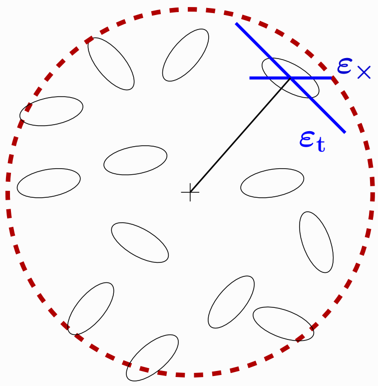

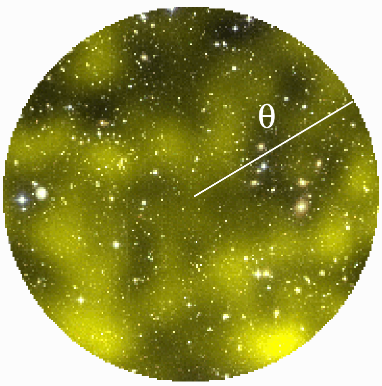

It is clear that $M_{\rm ap}$ ($M_\times$) is sensitive to the E-mode (B-mode) of the shear field γ.

When chosing Q such that its support is finite, with $Q(\theta) = 0$ for $\theta > \theta_{\rm max}$, the E-/B-mode separation is achieved on a finite interval.

To get this separation at the second-order level, let's take the variance of the aperture-mass: Square $M_{\rm ap}(\theta, \boldsymbol{\vartheta})$ and average over circle centres $\boldsymbol{\vartheta}$ (Schneider et al. 1998).

E-/B-mode separation with $M_{\rm ap}$ II

Square $M_{\rm ap}(\theta, \boldsymbol{\vartheta})$ and average over circle centres $\boldsymbol{\vartheta}$:

$$
\begin{aligned}
\langle M_{\rm ap}^2 \rangle(\theta) &= \int \mathrm{d}^2\vartheta' \, U_\theta(|\boldsymbol{\vartheta} - \boldsymbol{\vartheta}'|) \int \mathrm{d}^2\vartheta'' \, U_\theta(|\boldsymbol{\vartheta} - \boldsymbol{\vartheta}''|) \langle \kappa^{\rm E}(\boldsymbol{\vartheta}') \kappa^{\rm E}(\boldsymbol{\vartheta}'') \rangle \\
&= \int \mathrm{d}^2\vartheta' \, U_\theta(\vartheta') \int \mathrm{d}^2\vartheta'' \, U_\theta(\vartheta'') \langle \kappa^{\rm E} \kappa^{\rm E} \rangle(|\boldsymbol{\vartheta}' - \boldsymbol{\vartheta}''|) \\
&= \int \mathrm{d}^2\vartheta \, U_\theta(\vartheta) \int \mathrm{d}^2\vartheta' \, U_\theta(\vartheta') \\
&\quad \times \int \frac{\mathrm{d}^2\ell}{(2\pi)^2} \mathrm{e}^{-2\mathrm{i}\boldsymbol{\ell}\boldsymbol{\vartheta}} \int \frac{\mathrm{d}^2\ell'}{(2\pi)^2} \mathrm{e}^{2\mathrm{i}\boldsymbol{\ell}\boldsymbol{\vartheta}'} (2\pi)^2 \delta_{\rm D}(\boldsymbol{\ell} - \boldsymbol{\ell}') P_\kappa^{\rm E}(\ell) \\
&= \int \frac{\mathrm{d}^2\ell}{(2\pi)^2} \left(\int \mathrm{d}^2\vartheta \, \mathrm{e}^{2\mathrm{i}\boldsymbol{\ell}\boldsymbol{\vartheta}} U_\theta(\vartheta) \right)^2 P_\kappa^{\rm E}(\ell) \\
&= \frac{1}{2\pi} \int \mathrm{d}\ell \, \ell \, \hat{U}^2(\theta\ell) P_\kappa^{\rm E}(\ell).
\end{aligned}
$$

Note: Typically, the filter function U depends on the scale ϑ normalized to the radius θ, $U_\theta(\vartheta) = U(\vartheta/\theta)$. In Fourier space this then becomes $\hat{U}(\theta\ell)$.

E-/B-mode separation with $M_{\rm ap}$ III

For popular choices of U, $\hat{U}^2$ is a narrow pass-band filter function.

	polynomial	Gaussian
$U_\theta(\vartheta)$	$\begin{cases} \frac{9}{\pi\theta^2}\left(1 - \frac{\vartheta^2}{\theta^2}\right)\left(\frac{1}{3} - \frac{\vartheta^2}{\theta^2}\right) & \lvert\vartheta\rvert < \theta \\ 0 & \text{else} \end{cases}$	$\frac{1}{2\pi\theta^2}\left(1 - \frac{\vartheta^2}{2\theta^2}\right) \exp\left(-\frac{\vartheta^2}{2\theta^2}\right)$
$Q_\theta(\vartheta)$	$\begin{cases} \frac{6}{\pi\theta^2}\frac{\vartheta^2}{\theta^2}\left(1 - \frac{\vartheta^2}{\theta^2}\right) & \lvert\vartheta\rvert < \theta \\ 0 & \text{else} \end{cases}$	$\frac{\vartheta^2}{4\pi\theta^4} \exp\left(-\frac{\vartheta^2}{2\theta^2}\right)$
$\hat{U}(\eta)$	$\frac{24 \mathrm{J}_4(\eta)}{\eta^2}$	$\frac{\eta^2}{2} \exp\left(\frac{-\eta^2}{2}\right)$

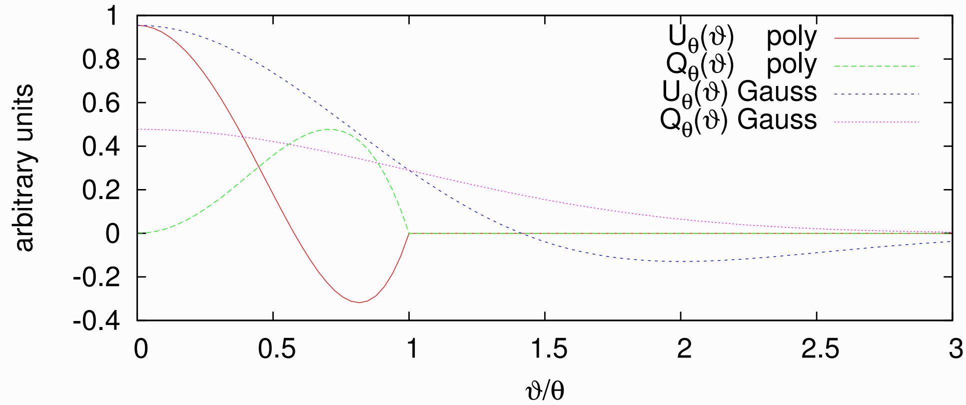

E-/B-mode separation with $M_{\rm ap}$ IV

Filter functions in Fourier space:

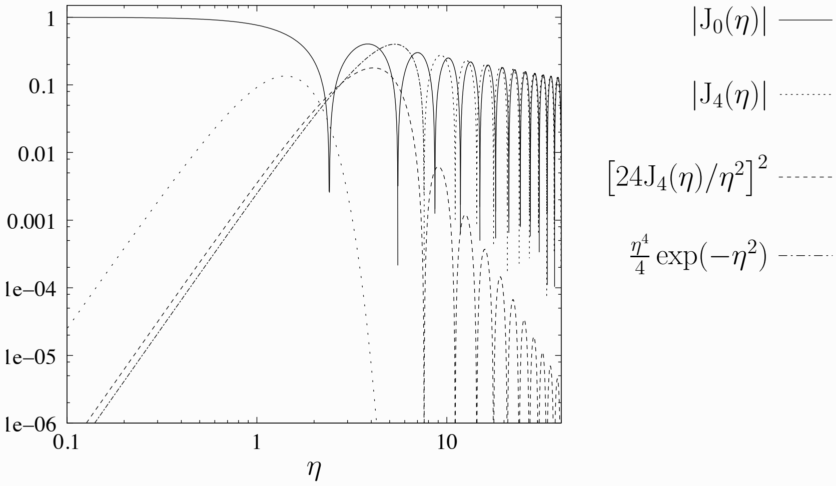

E-/B-mode separation with $M_{\rm ap}$ V

Thus, the aperture-mass dispersion filters out a small range of ℓ-modes around $\ell \sim \mathrm{const}\, \theta^{-1}$.

For example, for the polynomial filter from (Schneider et al. 1998), the peak is $\theta\ell \approx 5$.

Analogous equations for B- and mixed modes are

$$\langle M_\times^2 \rangle(\theta) = \frac{1}{2\pi} \int \mathrm{d}\ell\, \ell\, \hat U^2(\theta\ell) P_\kappa^{\rm B}(\ell);$$

$$\langle M_{\rm ap} M_\times \rangle(\theta) = \frac{1}{2\pi} \int \mathrm{d}\ell\, \ell\, \hat U^2(\theta\ell) P_\kappa^{\rm EB}(\ell).$$

In complex notation, the last three expressions can be written as

$$\langle M_{\rm ap}^2 \rangle(\theta) \pm \langle M_\times^2 \rangle(\theta) + 2\mathrm{i}\langle M_{\rm ap} M_\times \rangle(\theta) = \frac{1}{2\pi} \int \mathrm{d}\ell\, \ell\, \hat U^2(\theta\ell) \left[P_\kappa^{\rm E} \pm P_\kappa^{\rm B} + 2\mathrm{i} P_\kappa^{\rm EB} \right](\ell).$$

Aperture-mass dispersion and 2PCF I

The above recipe to get the aperture-mass variance can be implemented in an estimator as follows: For an aperture with center $\boldsymbol{\vartheta}$ and radius θ, average the observed galaxy ellipticities weighted by the filter Q. Square, average over many centers $\boldsymbol{\vartheta}$:

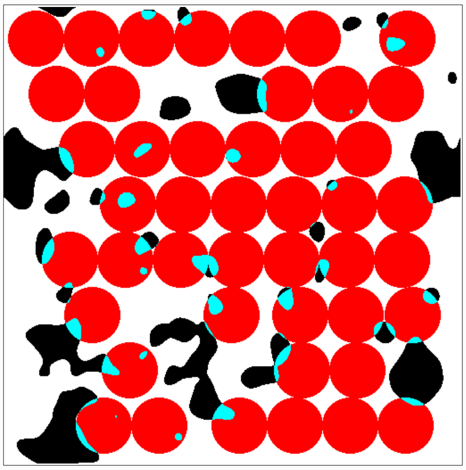

From [P. Simon, PhD thesis, 2005].

This is however not very efficient due to masked regions and field boundaries.

Solutions:

- Inpainting of missing data (Starck et al. 2006), using fast algorithms for convolution (Leonard et al. 2012).
- Compute 2PCF first, integrate to get aperture-mass dispersion.

Aperture-mass dispersion and 2PCF II

Aperture-mass dispersion from 2PCF

$M_{\rm ap}$ depends on $\gamma_{\rm t}$, thus we expect that $\langle M_{\rm ap}^2 \rangle$ depends on $\langle \gamma_{\rm t} \gamma_{\rm t} \rangle \sim$ 2PCF.
Simple calculation: Use

$$\langle M_{\rm ap}^2 \rangle(\theta) = \frac{1}{2\pi} \int {\rm d}\ell \, \ell \, \hat{U}^2(\theta\ell) P_\kappa^{\rm E}(\ell)$$

and insert

$$P_\kappa^{\rm E}(\ell) = \pi \int_0^\infty {\rm d}\vartheta \, \vartheta \left[\xi_+(\vartheta) {\rm J}_0(\ell\vartheta) + \xi_-(\vartheta) {\rm J}_4(\ell\vartheta) \right].$$

Result:

$$\langle M_{\rm ap}^2 \rangle(\theta) = \int_0^{2\theta} {\rm d}\vartheta \, \vartheta \left[T_+ \left(\frac{\vartheta}{\theta} \right) \xi_+(\vartheta) + T_- \left(\frac{\vartheta}{\theta} \right) \xi_-(\vartheta) \right].$$

with

$$T_\pm(x) = \int_0^\infty {\rm d}t \, t \, {\rm J}_{0,4}(xt) \hat{U}^2(t).$$

Aperture-mass dispersion and 2PCF III

The functions $T_\pm(x)$ have support $[0; 2]$, thus the above integral extends to 2θ. Therefore, the maximum distance to compute the shear correlation $\xi_\pm$ is $\vartheta_{\rm max} = 2\theta$.
Remember the diagram from Part I?

$$\begin{tikzcd}
\boldsymbol{\gamma} \text{ map} \arrow[r, "\text{filter with}", "Q"'] \arrow[d, "\substack{\text{sum over pairs}\\ \text{(auto-correlation)}}"'] & M_{\rm ap,\perp} \text{ maps} \arrow[d, "\sigma^2"] \\
\xi_\pm \arrow[r, "\text{filter with}", "T_\pm"'] & \langle M_{\rm ap}^2 \rangle, \langle M_\perp^2 \rangle
\end{tikzcd}$$

Maybe this makes a bit more sense now. . .

Aperture-mass dispersion measurements

CFHTLS 2007 versus CFHTlenS 2013.

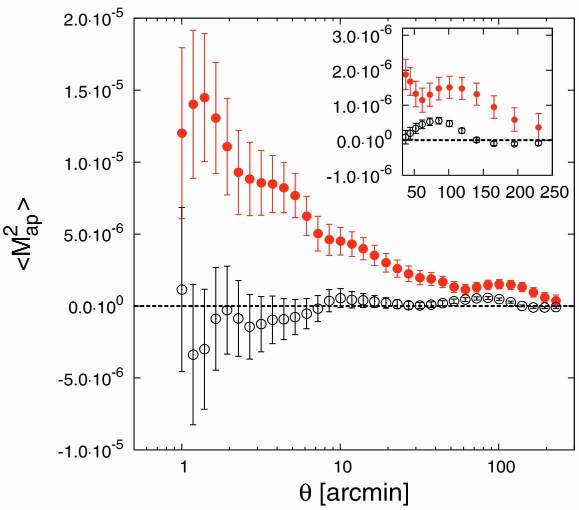

From (Fu et al. 2008).

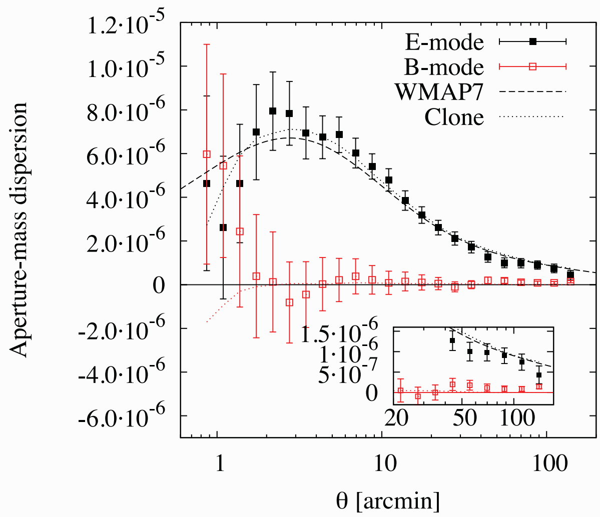

From (Kilbinger et al. 2013).

Ring statistic I

The problem of the unaccessible zero lag shear correlation for an E- and B-mode decomposition remains. How can we construct a E-/B-mode second-order correlation with a minimum galaxy separation $\vartheta_{\rm min} > 0$?

Solution: Correlate shear on two concentric rings (Schneider & Kilbinger 2007).
What are the minimum and maximum distances in this configuration?

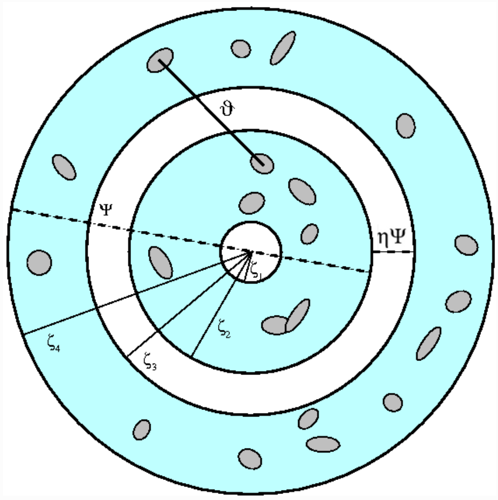

Figure from (Eifler et al. 2010).

Ring statistic II

Filter functions (in the original paper called $Z_\pm$ instead of $T_\pm$) depend on geometry of circles, and free-to-choose weight functions over the rings.

$$\langle \mathcal{R}\mathcal{R} \rangle_{\rm E,B} = \int_\eta^1 \frac{{\rm d}x}{2x} \left[\xi_+(x\Psi)\, T_+(x, \eta) \pm \xi_-(x\Psi)\, T_-(x, \eta) \right].$$

where $\eta = \vartheta_{\rm min}/\vartheta_{\rm max} < 1$ is ratio of minimum to maximum separation of the configuration.

General E-/B-mode decomposition on a finite interval (in $\log \vartheta$).
(Schneider & Kilbinger 2007) worked out the conditions on $T_\pm$ to have finite support, with $0 < \vartheta_{\rm min} < \vartheta_{\rm max} < \infty$:

$$\int_{\vartheta_{\rm min}}^{\vartheta_{\rm max}} {\rm d}\vartheta\, \vartheta\, T_+(\vartheta) = 0 = \int_{\vartheta_{\rm min}}^{\vartheta_{\rm max}} {\rm d}\vartheta\, \vartheta^3\, T_+(\vartheta)\,;$$

$$\int_{\vartheta_{\rm min}}^{\vartheta_{\rm max}} \frac{{\rm d}\vartheta}{\vartheta}\, T_-(\vartheta) = 0 = \int_{\vartheta_{\rm min}}^{\vartheta_{\rm max}} \frac{{\rm d}\vartheta}{\vartheta^3}\, T_-(\vartheta)\,.$$

Ring statistic measurements

CFHTLS 2007 versus CFHTLenS 2013.

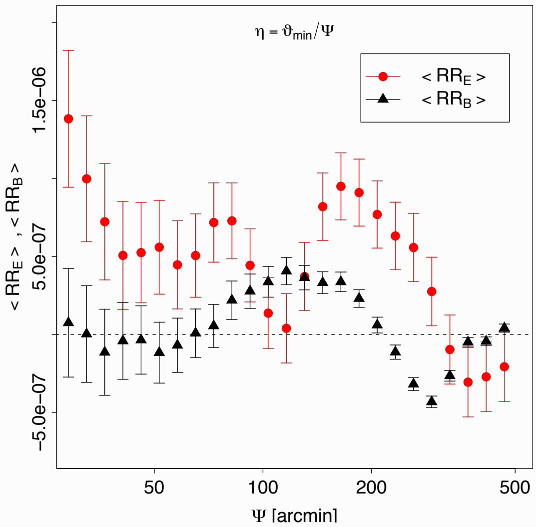

From (Eifler et al. 2010).

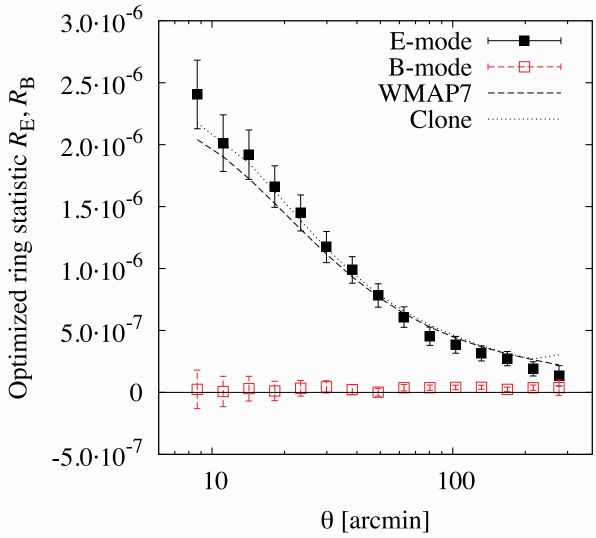

From (Kilbinger et al. 2013), optimised ring statisc following (Fu & Kilbinger 2010).

COSEBIs I

$$\int_{\vartheta_{\rm min}}^{\vartheta_{\rm max}} {\rm d}\vartheta \, \vartheta \, T_+(\vartheta) = 0 = \int_{\vartheta_{\rm min}}^{\vartheta_{\rm max}} {\rm d}\vartheta \, \vartheta^3 \, T_+(\vartheta) \; ;$$

$$\int_{\vartheta_{\rm min}}^{\vartheta_{\rm max}} \frac{{\rm d}\vartheta}{\vartheta} \, T_-(\vartheta) = 0 = \int_{\vartheta_{\rm min}}^{\vartheta_{\rm max}} \frac{{\rm d}\vartheta}{\vartheta^3} \, T_-(\vartheta) \; .$$

Under these conditions the functions $T_\pm$ can be freely choosen. Idea of (Schneider et al. 2010): Define modes E_n, B_n using polynomials of order $n+1$. Define family of orthogonal polynomials that provide all information about E-/B-modes on finite interval:

Complete Orthogonal Set of E-/B-mode Integrals.

The COSEBIs contain nearly all information that is in ξ_+ and ξ_-, except the very large scales. These are outside the survey, and cannot be decomposed into E-/B-modes, but form an ambigous mode. This mode is contained in $\xi_+(\theta)$, for which the filter $\mathrm{J}_0(\theta\ell) \to$ const for arbitrarily large $\ell \to 0$.

COSEBIs II

Polynomials can be linear in θ (Lin-COSEBIs), or linear in $z = \log\theta$ (Log-COSEBIs).

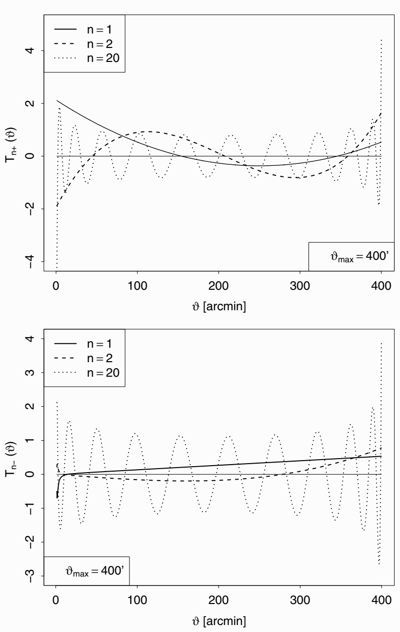

COSEBI linear filter functions $T_{\pm n}$ in real space.

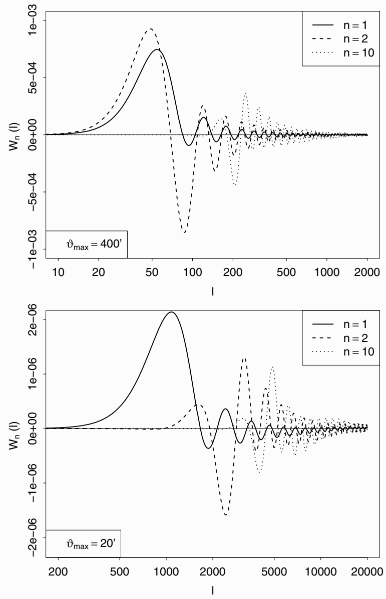

COSEBI linear filter functions W_n $(= \hat{U}^2)$ in Fourier space. From (Schneider et al. 2010).

COSEBIs III

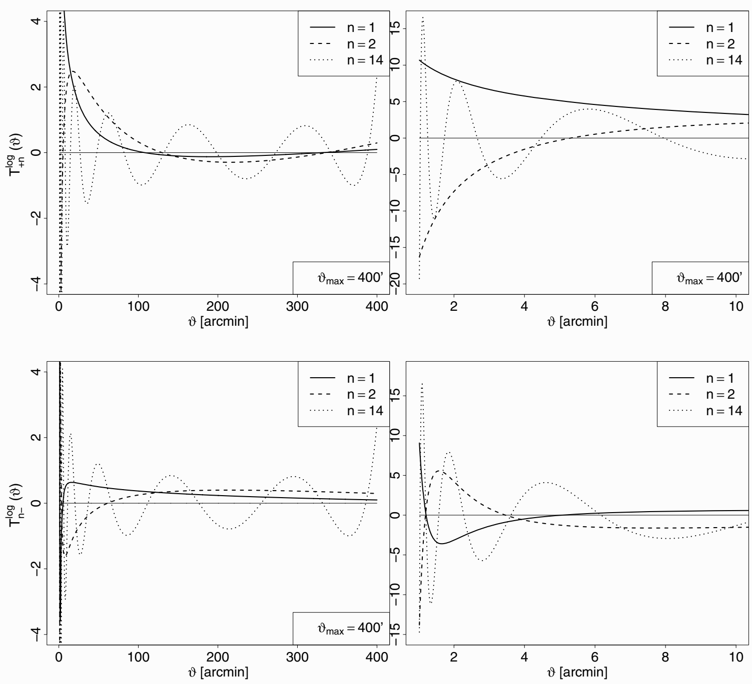

COSEBI logarithmic filter functions $T_{\pm n}$ in real space.

COSEBIs IV

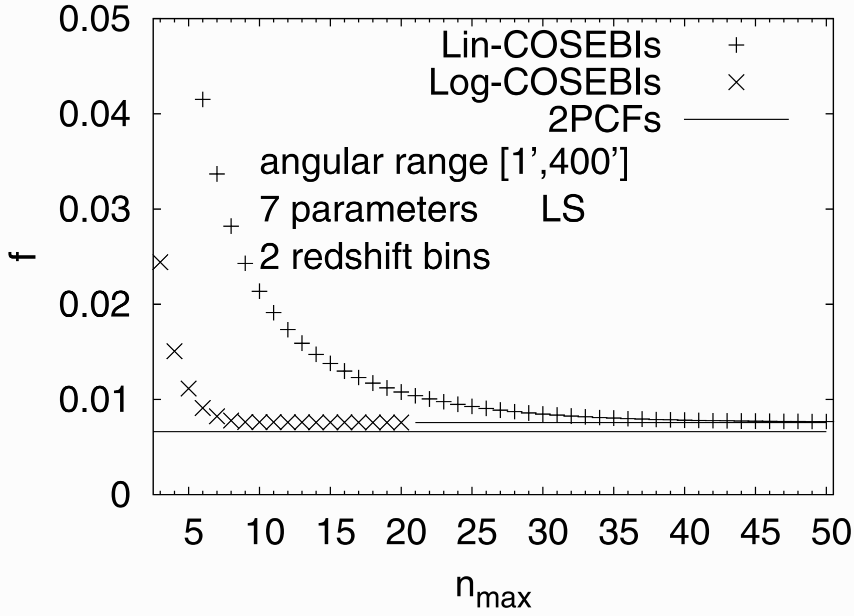

Inverse Fisher-matrix (allowed parameter) volume as function of COSEBIs maximum mode. From (Asgari et al. 2012).

Log-COSEBIs show faster convergence of available information with n.

Band-power spectrum I

The power spectrum P_κ can be estimated from shear data using methods from the CBM,
(Pseudo-C_ℓ, Bayesian, ...)
from pixellised maps.

A much faster but biased method is a band-power estimate from the 2PCF.

Recall the expressions

$$P_\kappa^{\rm E}(\ell) = \pi \int_0^\infty {\rm d}\vartheta \, \vartheta \, [\xi_+(\vartheta) {\rm J}_0(\ell\vartheta) + \xi_-(\vartheta) {\rm J}_4(\ell\vartheta)] \, ,$$
$$P_\kappa^{\rm B}(\ell) = \pi \int_0^\infty {\rm d}\vartheta \, \vartheta \, [\xi_+(\vartheta) {\rm J}_0(\ell\vartheta) - \xi_-(\vartheta) {\rm J}_4(\ell\vartheta)] \, .$$

To estimate these improper integrals as direct sums over observed $\xi_\pm$ between $\vartheta_{\rm min}$ and $\vartheta_{\rm max}$ would introduce large biases.

Band-power spectrum II

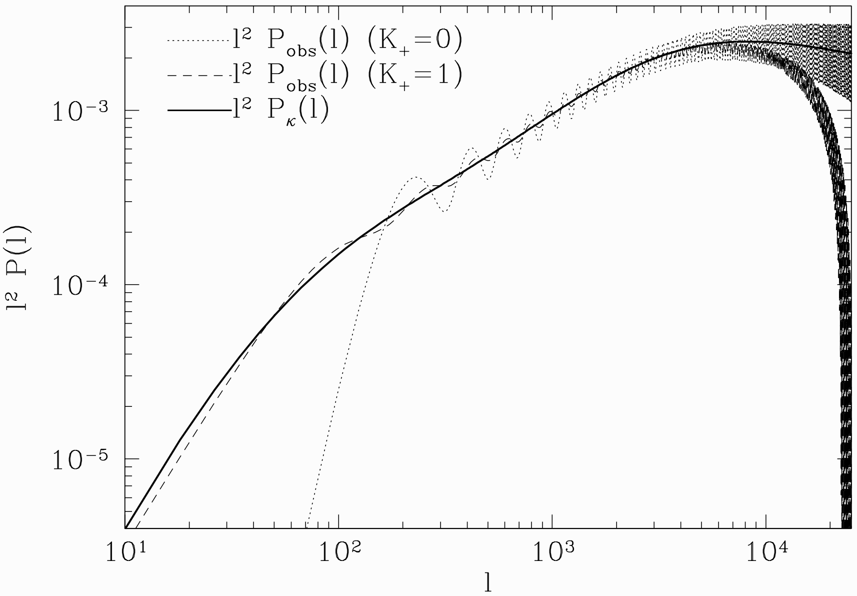

$$\hat{P}(\ell) = 2\pi \int_{\theta_{\min}}^{\theta_{\max}} \mathrm{d}\theta\, \theta\, \left[K_+ \xi_+(\theta) \mathrm{J}_0(\ell\theta) + (1-K_+)\xi_-(\theta)\mathrm{J}_4(\ell\theta)\right]$$

From (Schneider et al. 2002).

Band-power spectrum III

However, we can add another integration in bands of ℓ, between $\ell_{\min}$ and $\ell_{\max}$,

$$\mathcal{P}_i := \frac{1}{\Delta_i} \int_{\ell_{il}}^{\ell_{iu}} \mathrm{d}\ell\, \ell\, \hat{P}(\ell) = \frac{2\pi}{\Delta_i} \int_{\theta_{\min}}^{\theta_{\max}} \frac{\mathrm{d}\theta}{\theta} \left\{ K_+ \xi_+(\theta) \Big[g_+(\ell_{iu}\theta) - g_+(\ell_{il}\theta) \Big] + (1-K_+)\xi_-(\theta) \Big[g_-(\ell_{iu}\theta) - g_-(\ell_{il}\theta) \Big] \right\}$$

where $\Delta_i = \ln(\ell_{iu}/\ell_{il})$ is the logarithmic width of the band, and

$$g_+(x) = x\mathrm{J}_1(x) \quad ; \quad g_-(x) = \left(x - \frac{8}{x}\right)\mathrm{J}_1(x) - 8\mathrm{J}_2(x)\,.$$

This strongly reduces the bias.

You will use the program `pallas.py` in the TD this afternoon that implements this estimator.

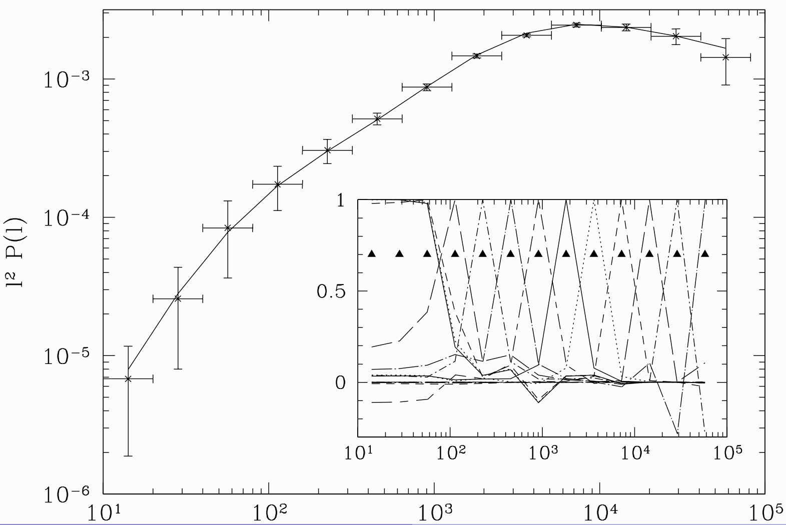

Galaxy-galaxy lensing: Overview

Correlation between high-z galaxy shapes and low-z galaxy positions.
E.g. average tangential shear around massive galaxies.
Provides mass associated with galaxy sample.

- Galaxy halo profiles from kpc to Mpc
- Mass-to-light ratio

In combination with other tracers of matter (galaxy clustering, cosmic shear, velocity correlations, X-ray emission, . . .):

- Galaxy bias. Properties such as linearity, scale-dependence, stochasticity
- Test of General Relativity

Can be done quasi model-independent since two or more observables trace same matter field, but with different biases.

Tangential shear and projected overdensity

Tangential shear at distance θ is related to total overdensity within this radius:

$$\langle \gamma_{\rm t} \rangle (\theta) = \bar\kappa(\le \theta) - \langle \kappa \rangle (\theta).$$

No assumption about mass distribution is made here!

End of day 1.